Sexual dimorphism of *STGC3* tumor suppressor function in nasopharyngeal carcinoma CNE2 cells

Q. Qiu[1,2]*, B. Hu[1,2,4]*, Z.C. Chen[3] and X.S. He[1]

[1]Cancer Research Institute, University of South China, Hengyang, Hunan, China
[2]Department of Medicine, Vanderbilt University, Nashville, TN, USA
[3]Cancer Research Institute, Central South University, Changsha, Hunan, China
[4]Hunan Environment-Biological Polytechnic College, Hengyang, Hunan, China

*These authors contributed equally to this study.
Corresponding authors: X.S. He / Z.C. Chen
E-mail: hexiusheng@hotmail.com / tcbl@xysm.net

ABSTRACT. *STGC3* is a potential tumor suppressor in nasopharyngeal carcinoma. We previously found that CNE2 cells that re-expressed *STGC3* formed smaller tumors in female mice than in male mice. Here, we investigated the sexual dimorphism of *STGC3* as a tumor-suppressor in female and male nude mice injected subcutaneously with pcDNA3.1(+)-*STGC3*/CNE2 cells. ER-α was positively expressed *in vitro* in the CNE2 cells. The pcDNA3.1(+)-*STGC3*/CNE2 cell growth rate decreased after treatment with β-estradiol *in vitro*. There were significant differences in tumor size or mass between pcDNA3.1(+)-*STGC3*/CNE2 and control cases (P < 0.05), but there were significant differences in tumor size between female and male nude mice in the *STGC3* transfection groups, and the pcDNA3.1(+)-*STGC3*/CNE2 tumor growth rate in the female nude mice was the lowest in all cases (P < 0.05). There were no significant differences between female

and male nude mice in control groups. Furthermore, a greater number of cells were blocked in the G_0/G_1 phase in pcDNA3.1(+)-*STGC3*/CNE2 tumor xenografts in the female mice. Protemic analysis found 9 differentially expressed proteins in the pcDNA3.1-*STGC3*/CNE2 xenograft tissues in females and males. A heat shock 70 protein 8 isoform 2 variant was identified as a down-regulated protein associated with cell cycle control and its downstream factor cyclin D1 was also decreased in *STGC3*-repressed xenografts in female mice. The data above suggest that *STGC3* and its associated proteins play an important role in nasopharyngeal carcinoma gender differences.

Key words: Nasopharyngeal carcinoma; STGC3; CNE2 cell line; Sexual dimorphism

INTRODUCTION

Nasopharyngeal carcinoma (NPC) is one of the most common malignant tumors in Southeast Asia and southern China (Xiong et al., 2004; Wang et al., 2011). The crucial etiologic factors involved in NPC include the Epstein-Barr virus, chemical carcinogens, radiation, structural or functional mutation of oncogenes and tumor suppressor gene, and chromosomal aberrations (Chong and Ong, 2008). NPC accounts for 0.25% of all malignancies in the United States and 15-18% of malignancies in southern China. It also accounts for 10-20% of childhood malignancies in Africa (Abdel Khalek Abdel and King, 2012). The incidence of NPC is higher in men than in women. For most populations, the male to female incidence ratio is roughly 3:1 (Yu and Yuan, 2002; Chong and Ong, 2008; Abdel Khalek Abdel and King, 2012).

STGC3 is a novel gene that was cloned by our group. It is related to NPC (He et al., 2004). Our previous research showed that the expression of *STGC3* was diminished or even deleted in NPC cell lines and tissues. Restoring the expression of *STGC3* in CNE2 cells significantly inhibits its growth and proliferation *in vitro* and *in vivo* (He et al., 2008; Qiu et al., 2012). This indicates that *STGC3* is a candidate tumor suppressor in NPC (He et al., 2004, 2008; Li et al., 2011; Qiu et al., 2012). Our experiments have also indicated that there is sexual dimorphism in the tumor inhibition effect of *STGC3*, with the gene's tumor suppressor effect being more prominent in female mice than in males. In 1966, Jessen elucidated the relationship between estrogen and tumors as a two-step mechanism of estradiol action in which association with the hormone converts a receptor from an inactive to an active form that will bind tightly in the nucleus to modify transcription (Jensen et al., 1968; Jensen, 1966, 2005). In this study, we explore the sexual dimorphism of *STGC3* tumor suppression in the CNE2 NPC cell line and identify proteins involved in the phenomenon.

MATERIAL AND METHODS

Cell culture

CNE2, a poorly differentiated NPC cell line, was cultured at 37°C with humidified 5% CO_2 in RPMI 1640 medium (Invitrogen, USA) supplemented with 10% fetal bovine serum.

Plasmid construction and transfection

To construct the recombinant plasmid pcDNA3.1-*STGC3*, the open reading frame of *STGC3* encoding the full-length protein was amplified by PCR using primers containing *Bam*HI and *Xho*I restriction sites. The PCR product was subcloned into the expression vector pcDNA3.1, which contains the hygromycin-resistance gene. The recombinant plasmid was confirmed by *Bam*HI/*Xho*I digestion and DNA sequencing. The pcDNA3.1 vector (Invitrogen) and the pcDNA3.1-*STGC3* vector were transferred to CNE2 cells using the Lipofectamine 2000 protocol (Invitrogen). The positive clones were identified and selected for further development, and then cultured with a 200 μg/mL G418 solution to maintain resistance. The expression of *STGC3* was confirmed by RT-PCR and Western blotting.

Nude mice experiment

Three-week-old BALB/c nude mice were acquired from the Animal Centre of Academia Sinica in Shanghai (China). All animal experiments were approved by the National Animal Care and Use Committee of China and carried out 1 week after the arrival of the nude mice.

Twelve female and 12 male nude mice were randomly divided into 6 groups: CNE2/male (CNE2/M, 4 mice), CNE2/female (CNE2/F, 4 mice), pcDNA3.1(+)/CNE2/male (Vector/M, 4 mice), pcDNA3.1(+)/CNE2/female (Vector/F, 4 mice), pcDNA3.1(+)-*STGC3*/CNE2/male (*STGC3*/M, 4 mice), and pcDNA3.1(+)-*STGC3*/CNE2/female (*STGC3*/F, 4 mice). The 3 types of cells were trypsinized and cell suspensions were prepared. A 0.2-mL (2×10^6 cells) cell suspension was inoculated under the right armpit of each nude mouse. The tumor growth rate was monitored by measuring 2 diameters at right angles with vernier calipers every 3 days. The tumor volumes were calculated using the formula: $W^2 \times L \times 0.52$, where *L* is the length and *W* is the width of the tumor. The mean value of tumor size in each group was plotted. The inhibition ratio (%) = (mean of the vector group) - (mean of the transfected group) / (mean of the vector group) x 100.

Histology and immunohistochemistry

The subcutaneous tumors containing different cells were excised from the nude mice under ether inhalation anesthesia. The tumors were fixed overnight at 4°C in 4% formaldehyde and embedded in paraffin. Paraffin sections (5 μm) were stained with hematoxylin and eosin (H&E). Immunohistochemistry was performed as previously described (He et al., 2008) or with estrogen receptor α (ERα, 1:100, Santa Cruz Biotechnology, USA). Primary antibodies were rabbit anti-STGC3 (1:100) (He et al., 2008). Biotinylated secondary antibody was from Santa Cruz Biotechnology (1:500). The antibody staining was imaged using an Axioscope 40 microscope (Zeiss) equipped with an Axiocam HRc camera (Zeiss).

RNA extraction and RT-PCR

Total RNA was isolated from xenograft tissues using the Trizol reagent (Invitrogen) according to manufacturer instructions. A total of 2 μg DNase-treated RNA was reverse transcribed into first-strand cDNA using the SuperScript First-Strand Synthesis System for RT-

PCR (Promega, USA) with random hexanucleotide primers. cDNA (2 μL) for *STGC3* was amplified with the following primers: forward 5'-CGG GAT CCA TGG TTC TTG TTT CTT AT-3' and reverse 5'-GCC CCA AGC TTT AGA GTA ATA AAA GAT TC-3'. PCR was performed for 30 cycles, each consisting of denaturation at 94°C for 1 min, annealing at 56°C for 50 s, and extension at 72°C for 1 min. β-actin (forward primer, 5'-GGA CCT GAC TGA CTA CCT C-3' and reverse primer, 5'-CAT ACT CCT GCT TGC TGA T-3') was amplified to confirm an equal amount of total mRNA in samples and was used to normalize samples.

Protein extraction and Western blotting

Xenograft tissues were extracted in lysis buffer (0.5% Nonidet P-40, 5% sodium deoxycholate, 50 μM NaCl, 10 μM Tris-HCl, pH 7.5, 1% BSA) and centrifuged at 4°C for 15 min. The supernatant was mixed with 2X loading buffer and boiled for 5 min, and then the samples were separated using 10% gradient SDS/PAGE gels and transferred to PVDF membranes. The membranes were blotted with 5% fat-free milk at room temperature for 1 h, incubated at 4°C overnight with anti-STGC3 (1:1000) (He et al., 2008), anti-HSP70 (1:500), anti-cyclin D1 (1:1000), and anti-β-actin (1:5000; Santa Cruz Biotechnology), washed, and then incubated with peroxidase-conjugate secondary Ab (1:3000; Santa Cruz Biotechnology). Detection of immunoreactivity was performed by enhanced chemiluminescence (Amersham Biosciences, Sweden).

Flow cytometry

Cell suspensions were prepared from the 6 groups of xenograft tumor tissues. These were centrifuged, diluted to 1×10^6 cells/mL, fixed in 70% ethanol, and stored in fixative at -20°C until prepared for cell apoptosis analysis. Fixed cells were washed with PBS and incubated with propidium iodide (50 μg/mL in PBS) for 30 min at room temperature in the dark. Analysis of the DNA content in propidium iodide-stained cells was performed by flow cytometry.

Two-dimensional electrophoresis (2-DE)

2-DE was performed as described by the manufacturer (Amersham Biosciences). Protein samples (800 μg for preparative gels) were mixed with loading buffer for IPG strips to obtain a final volume of 450 μL. Next, isoelectric focusing was carried out on an IPGphor system using IPG strips (pH 3-10L, 24 cm, Amersham Biosciences). Second-dimension SDS-PAGE was performed on an Ettan DALT II system. After electrophoresis, Coomassie blue staining was used to visualize the protein spots in the 2-DE gels.

Image analysis

The stained 2-DE gels were scanned with the MagicScan software on an Imagescanner and analyzed by using a PD-Quest system (Bio-Rad Laboratories, USA) according to protocols provided by the manufacturer. The criteria to determine differential protein spot was that spot intensity increased or decreased more than 2-fold between the comparison groups.

MALDI-TOF-MS and database analysis

Protein spots of interest were excised from the preparative gel, destained, and in-gel trypsin digested. The tryptic peptides were mixed with 4-hydroxy-a-cyanocinnamic acid in 50% acetonitrile, 2.5% TFA and analyzed using a Voyager System 4307 MALDI-TOF-MS (ABI) to obtain the peptide mass fingerprint. Peptide matching and protein searches against the NCBI database were performed using the Mascot search engine (http://www.matrixscience.com/) with a mass tolerance of ±50 ppm.

Statistical analysis

Data are reported as means ± SD for at least 3 separate experiments. Statistical analysis was performed where appropriate using the Student *t*-test or one-way ANOVA followed by the Tukey multiple comparison test. $P < 0.05$ was considered to be statistically significant.

RESULTS

β-estradiol enhances the tumor inhibition effect of *STGC3 in vitro*

β-estradiol is the predominant estrogen during reproductive years both in terms of absolute serum levels and estrogenic activity, which is the main difference between female and male mammals. Before starting *in vivo* experiments, we examined whether β-estradiol enhances the effect of *STGC3* tumor inhibition on CNE2 cells in culture. ERα expression in CNE2 cells was confirmed by immunohistochemistry, which showed that ERα was expressed mainly in the nucleus of CNE2 cells (Figure 1A). The recombinant plasmid pcDNA3.1-*STGC3* was identified by restriction enzyme digest with *Bam*HI and *Xho*I and DNA sequencing (Figure 2A), and then pcDNA3.1 or pcDNA3.1-*STGC3* plasmids were transferred to the CNE2 cells. Four of 24 pcDNA3.1-*STGC3* clones and 3 pcDNA3.1 clones were identified with RT-PCR and Western blotting (Figure 2B and C, respectively). The growth curves and cell cycle distribution of the 4 pcDNA3.1-*STGC3* clones were very similar. We chose the clone with the strongest *STGC3* expression, which was the number 5 clone. Growth curve and statistical analysis indicated that the growth rate of CNE2 cells transfected with *STGC3* was slower than that of the vector-transfected CNE2 controls ($P < 0.05$). One micromolar β-estradiol decreased the growth rate of *STGC3*-transfected CNE2 cells (Figure 1B, $P < 0.05$), which suggested that *STGC3* inhibits the proliferation of CNE2 cells and β-estradiol enhances the effect of *STGC3*.

The tumor inhibition effect of *STGC3* on CNE2 cells has a sexual dimorphism in nude mice

We speculated that the tumor inhibition effect of *STGC3* in the CNE2 line may exhibit sexual dimorphism *in vivo* because of the different level of β-estradiol production between the adult female and male mice. To test this hypothesis, CNE2, pcDNA3.1/CNE2, and pcDNA3.1-*STGC3*/CNE2 cells were injected subcutaneously in female and male nude mice (Figure 3A) and tumors were then subject to further evaluation. RT-PCR, Western blotting, and immunohistochemistry confirmed that *STGC3* was highly expressed in the pcDNA3.1-*STGC3*/CNE2 xenografts (Figure 4).
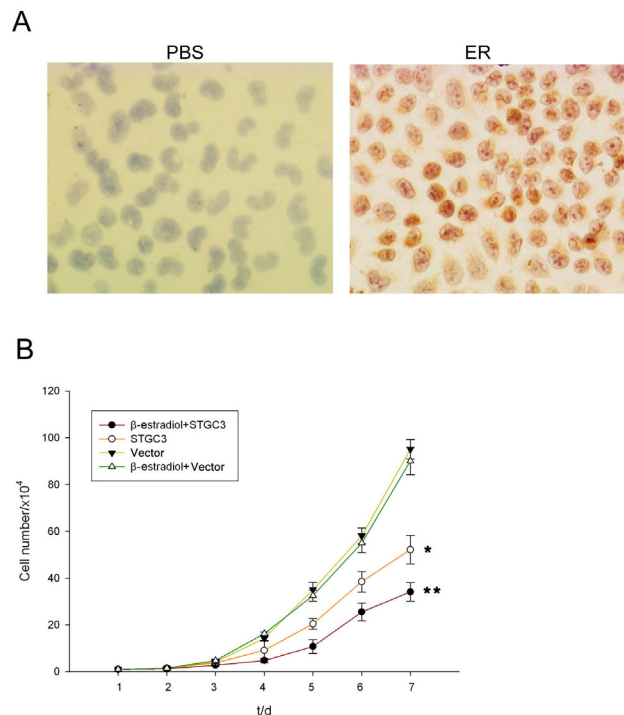
Figure 1. Inhibition effect of β-estradiol on the pcDNA3.1(+)-*STGC3*/CNE2 cell. **A.** ERα expression in CNE2 cells by immunohistochemistry (SP, 400X) (left: negative control, right: ERα staining). **B.** Growth curves of β-estradiol-treated pcDNA3.1(+)-*STGC3*/CNE2 cells. *P < 0.05 for pcDNA3.1(+)-*STGC3*/CNE2 compared with the pcDNA3.1(+)/CNE2 group. **P < 0.05 for β-estradiol-treated pcDNA3.1(+)-*STGC3*/CNE2 group compared with the untreated STGC3 group.
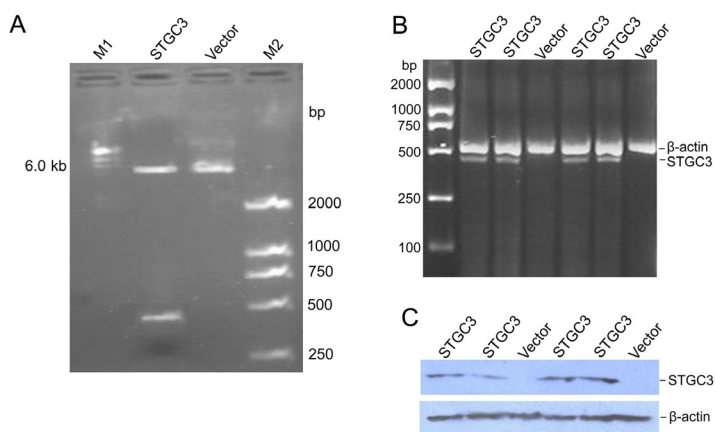

Figure 2. Selection of stable STGC3-expressed CNE2 cell line. **A.** Identification of recombinant by restriction endonuclease digestion with *Bam*HI and *Xho*I. **B.** *STGC3* mRNA detection in CNE2 cell lines by RT-PCR. **C.** Re-expression of the *STGC3* gene in CNE2 cells detected by Western blot.
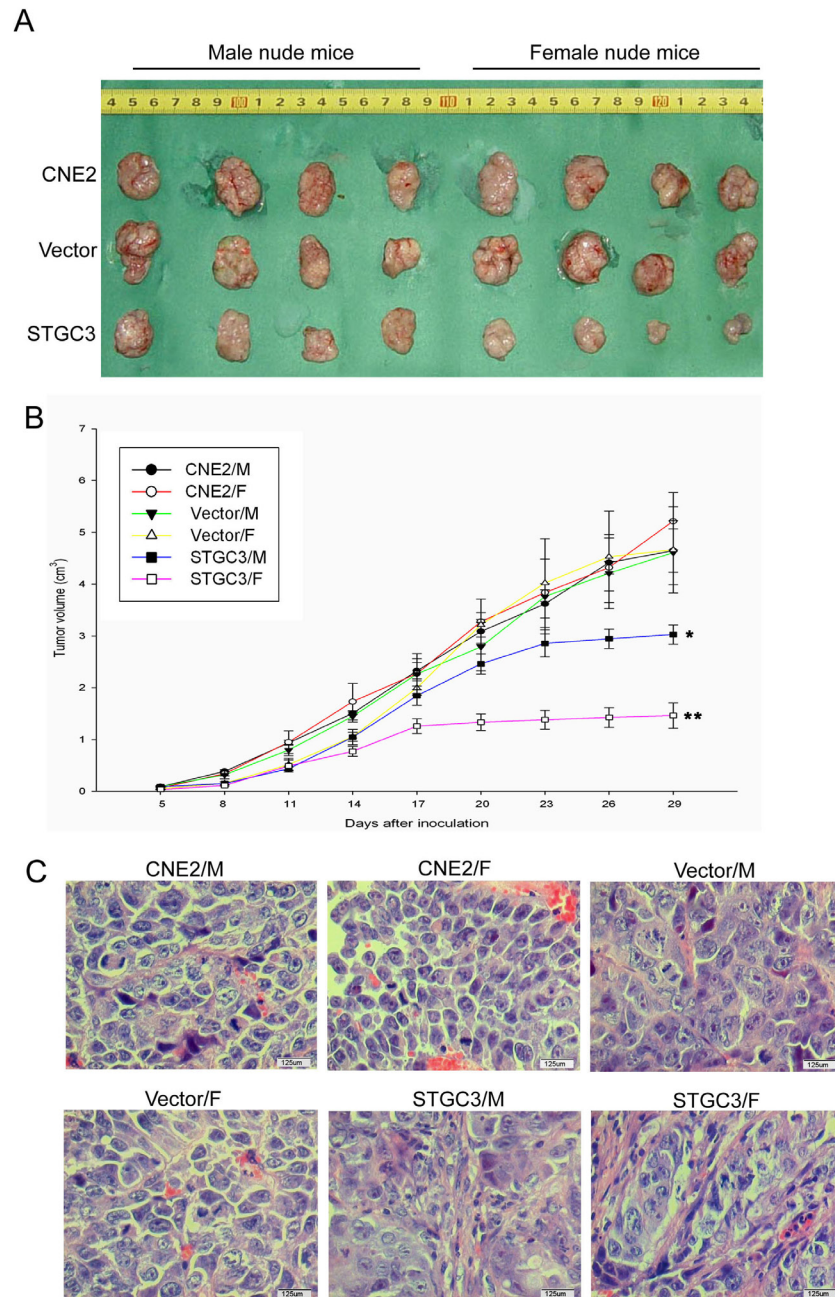
Figure 3. Over-expression of STGC3 inhibits tumor growth and increases differentiation in nude mice with a sexual dimorphism. **A.** Comparison of subcutaneously injected xenografts of nude mice. **B.** Time-volume curves for the xenografts. *P < 0.05 for *STGC3*/M compared with the Vector/M group. **P < 0.05 for *STGC3*/F compared with the *STGC3*/M group. **C.** Hematoxylin and eosin staining shows STGC3 increase differentiation in xenograft tissues.
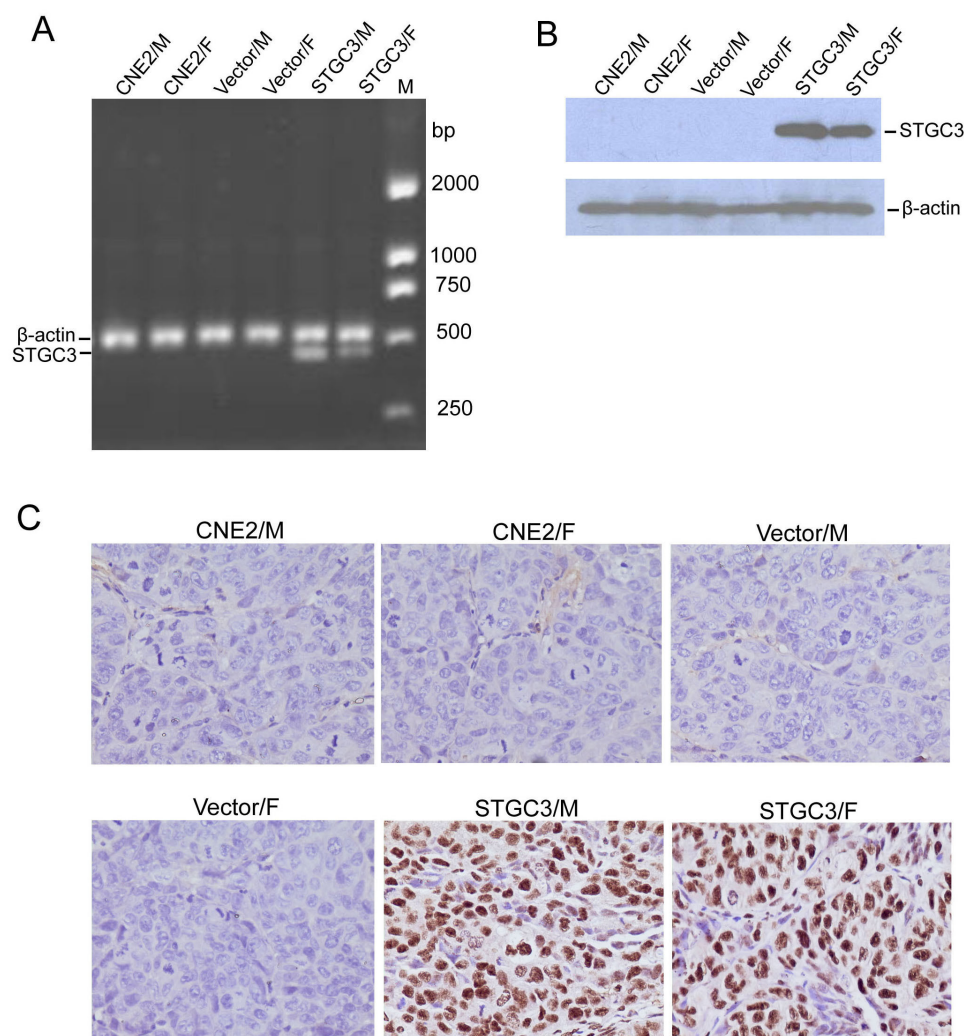
Figure 4. High level of *STGC3* expression in the pcDNA3.1(+)-*STGC3*/CNE2 cell line. **A.** RT-PCR analysis for *STGC3* mRNA expression in the xenograft tissues. **B.** Western blot analysis using an anti-STGC3 antibody consistent with the RT-PCR results. **C.** Immunohistochemistry staining of anti-STGC3 in the xenograft tissues.

Next, to determine whether *STGC3* inhibits tumor growth, we monitored the masses and volumes of the tumors. In male nude mice, the mass weights of xenografts of pcDNA3.1-*STGC3*/CNE2 tumors (*STGC3*/M) were smaller (3.024 ± 0.374 g) than those in the control groups CNE2/M (4.648 ± 0.840 g) and Vector/M (pcDNA3.1/CNE2: 4.610 ± 1.234 g) (Table 1). The xenograft growth suppression ratio of pcDNA3.1-*STGC3*/CNE2 to pcDNA3.1/CNE2 was as high as 35.2%. Time-volume curves for the xenografts showed that pcDNA3.1-*STGC3*/CNE2 tumors had slower growth rates than those of the 2 control groups in the male mice ($P < 0.05$) (Figure 3B).

Table 1. Comparison of volume and mass means of xenografts (N = 4, $\bar{\chi} \pm$ SD).

Groups	Tumor volumes (cm³)	Tumor weight (g)
CNE2/male	4.648 ± 0.840	3.18 ± 0.89
CNE2/female	5.216 ± 1.110	3.10 ± 0.40
pcDNA3.1(+)/CNE2/male	4.610 ± 1.234	3.65 ± 0.96
pcDNA3.1(+)/CNE2/female	4.662 ± 1.664	3.32 ± 0.54
pcDNA3.1(+)/STGC3/CNE2/male	3.024 ± 0.374	2.06 ± 0.41*
pcDNA3.1(+)/STGC3/CNE2/female	1.462 ± 0.490	0.99 ± 0.52**

*P < 0.05 as compared with the pcDNA3.1(+)/CNE2/male group. **P < 0.05 as compared with the pcDNA3.1(+)/STGC3/CNE2/male group. SD = standard deviation.

The mass weight of xenografts of pcDNA3.1-*STGC3*/CNE2 cells in female nude mice were smaller (1.462 ± 0.490 g) than those in male nude mice (3.024 ± 0.374 g) (Table 1). However, no sexual dimorphisms were noted in either the CNE2 or pcDNA3.1/CNE2 groups. These results again indicated that *STGC3* in the mouse model affects tumor growth in females more than males.

Our previous *in vitro* experiments with CNE2 cells showed that *STGC3* suppresses anchorage-independent cell growth on soft agar, signifying a tumor-suppressor role (He et al., 2008). Thus, we used our xenograft tissue to determine whether *STGC3* affects tumor malignancy *in vivo*. H&E staining showed that xenografts with high *STGC3* expression were better differentiated than those in the 2 control groups in the male mice. In the *STGC3* over-expression group, cells were characterized by smaller nuclei, more regular size and shape, less prominent nucleoli, and more abundant cytoplasm (Figure 3C). These results support the idea that over-expression of *STGC3* increases differentiation of CNE2 cells *in vivo*.

STGC3 increases the number of CNE2 cells in G_0/G_1 phase in females more than in males

To determine the molecular mechanism by which the over-expression of *STGC3* causes tumor inhibition *in vivo*, we examined the cell cycle distribution of the xenografts by flow cytometry. Compared to pcDNA3.1/CNE2 xenografts, pcDNA3.1-*STGC3*/CNE2 xenografts showed a significant increase of cell percentages in G_0/G_1 phase (31.6 ± 0.5 *vs* 41.7 ± 0.6, respectively; P < 0.01), and the percentage of *STGC3* xenograft cells arrested in G_0/G_1 was greater in the female nude mice (50.7 ± 0.7) than in the males (41.7 ± 0.6) (Table 2). The above results imply that sexual dimorphism of the effect of *STGC3* may be related to the G_0/G_1 cell cycle arrest.

Table 2. Up-regulated and down-regulated spots in pcDNA3.1(+)/*STGC3*/CNE2/F group.

Spot	Accession No.	Protein identify	Expressed in STGC3/F	MW	Match peptides	pI	Coverage sequence (%)
1	P07195	L-lactate dehydrogenase B chain	↓	36769	9/25	5.72	48
2	P63243	Guanine nucleotide-binding protein subunit beta 2-like 1	↓	35380	22/37	7.56	83
3	Q53HW2	Ribosomal protein P0 variant	↑	34423	13/31	5.71	58
4	Q5SY06	Fumarate hydratase	↑	54773	12/20	8.85	54
5	Q53HF2	Heat shock 70 protein 8 isoform 2 variant	↓	53580	14/57	5.62	39
6	A46711	Thioredoxin peroxidase	↑	22324	13/30	8.27	66
7	S06590	IgE-dependent histamine-releasing factor	↑	19697	9/24	4.84	77
8	P23528	Cofilin-1	↓	18588	6/20	8.26	53
9	AAO46160	Serine/threonine-protein kinase WNK1	↑	3805	3/9	6.51	83

MW = molecular weight; pI = isoelectric point.

Differential expression of proteins associated with sexual dimorphism of *STGC3* tumor suppression

Because the STGC3 protein is localized in the nucleus (Figure 4C), it probably acts chiefly in the nucleus, associated with regulation of gene transcription. The sexual dimorphism may be caused by translation of different genes. To test this hypothesis, we initiated a comparative proteomics study of the pcDNA3.1-*STGC3*/CNE2 xenograft tissues from female and male nude mice. Figure 5A shows representative examples of the xenograft tissue proteins separated on 2-DE gel. A total of 807 ± 18 and 843 ± 32 protein spots were detected in female and male pcDNA3.1-*STGC3*/CNE2 xenograft tissues, respectively. Consistently detected protein spots with expression changes greater than 2-fold were included in the analysis (Figure 5A and B).

The differentially expressed protein spots were excised from Coomassie brilliant blue-stained gels and subjected to in-gel digestion with trypsin. An aliquot of the supernatant containing tryptic peptides was analyzed by MALDI-TOF-MS (Figure 5C). Only the proteins ranked with a significant score on the Mascot database were identified as the differentially expressed proteins, so that finally 9 differentially expressed proteins between the female and male pcDNA3.1-*STGC3*/CNE2 xenograft tissues, and are labeled in Figure 5A. Detailed information about the 9 proteins is listed in Table 2, which contains the MSDB/NCBI accession code, matched peptides, pI, molecular weight, expression levels in female pcDNA3.1-*STGC3*/CNE2 xenograft tissues, and protein names.

To functionally characterize the proteins related to sexual dimorphism of *STGC3*, we searched for them on the Swiss-Prot and PubMed databases. The differential proteins involved in cell cycle regulation, such as heat shock 70 protein 8 (Hsc70) isoform 2 variant, were down-regulated (Powers et al., 2008), cytoskeleton proteins such as cofilin-1 up-regulated (Chae et al., 2009), cell metabolism proteins such as fumarate hydratase upregulated (Pollard et al., 2005), L-lactate dehydrogenase B chain down-regulated (Takatani et al., 2001), IgE-dependent histamine-releasing factor up-regulated (Yoneda et al., 2004), and signal pathways such as guanine nucleotide-binding protein subunit beta 2-like 1 down-regulated (Zhang et al., 2010) in the pcDNA3.1-*STGC3*/CNE2 xenograft tissues of the female nude mice.

***STGC3* increases cell cycle associated protein Hsc70 and cyclin D1**

To confirm the differential expression of the proteins that we identified by comparative proteomics, the expression levels of Hsc70 in the female and male pcDNA3.1-*STGC3*/CNE2 xenograft tissues were measured by Western blotting. Figure 5D shows the representative Western blot results for Hsc70 in the pcDNA3.1-*STGC3*/CNE2 xenograft tissues. The female pcDNA3.1-*STGC3*/CNE2 xenograft tissues exhibited an obvious 2/3 decrease of Hsc70. These results were identical with the data from 2-DE.

We also analyzed cyclin D1 expression in female and male pcDNA3.1-*STGC3*/CNE2 xenograft tissues, and cyclin D1 also decreased in pcDNA3.1-*STGC3*/CNE2 xenograft tissue compared with vector xenograft tissue (Figure 5D), and its expression was lower xenograft tissue from females than from males.
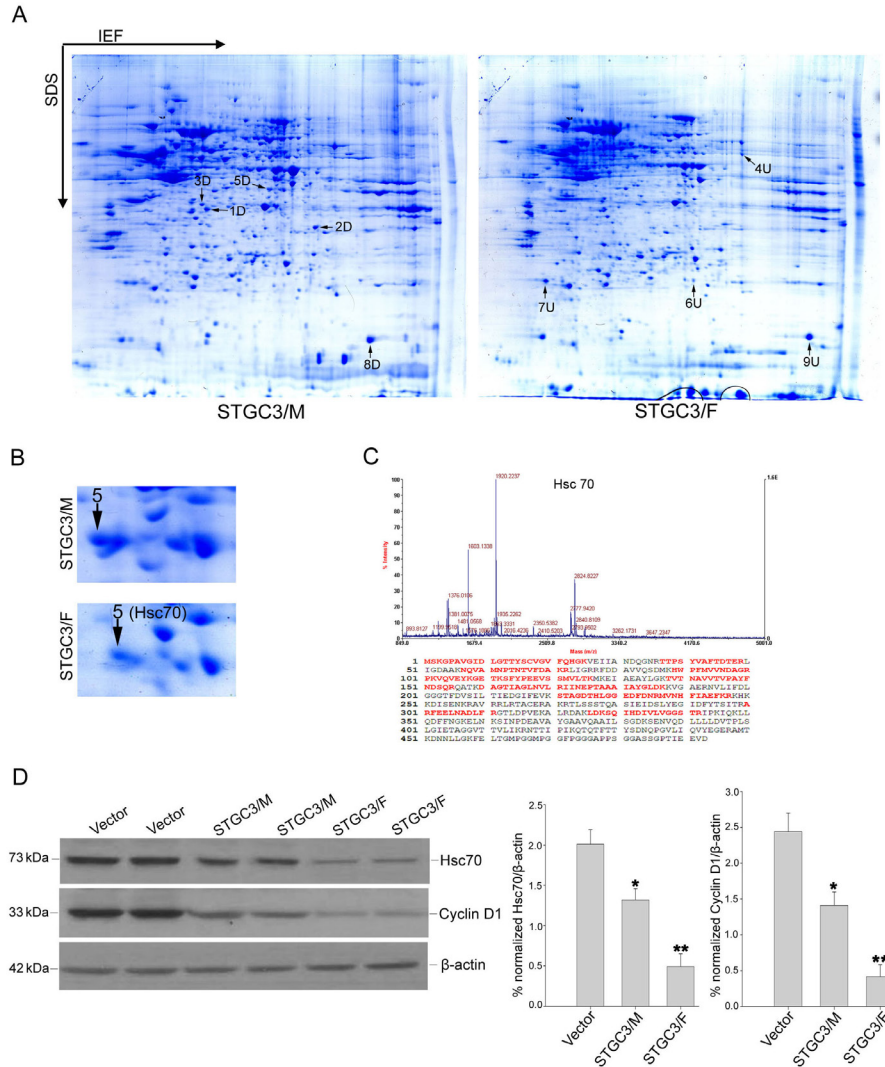
Figure 5. Comparative proteomic analysis of *STGC3*/M and *STGC3*/F xenograft tissues by 2-DE, MS and Western blot. **A.** 2-DE maps of *STGC3*/M and *STGC3*/F xenograft tissue proteins. **B.** A close-up of the region of 2-DE gel images showing the significant over-expression of protein spot 5 in *STGC3*/M compared with *STGC3*/F. **C.** MALDI-TOF-MS analysis of differential protein spot 5. **D.** Western blot analysis for Hsc70 and cyclin D1 expression in xenograft tissues. *$P < 0.05$ for *STGC3*/M compared with the Vector group. **$P < 0.05$ for *STGC3*/F compared with the *STGC3*/M group.

DISCUSSION

In this study, female and male mice received subcutaneous injections of pcDNA3.1-*STGC3*/CNE2 cells and *STGC3* was over expressed in the pcDNA3.1-*STGC3*/CNE2 xenografts. Details of this expression were examined, and tumor inhibition by *STGC3* exhibited

sexual dimorphism, which is consistent with the roughly 3:1 male:female ratio of NPC. Our results have also provided more evidence for the tumor suppressor role of STGC3 in the development and treatment of NPC.

In the cytometry experiments, *STGC3* increased the number of CNE2 cells in the G_0/G_1 phase, and there were fewer cells in S and M phases in female nude mice than in males. This implies that the sexual dimorphism of tumor inhibition by *STGC3* is related to its effect on expression of proteins associated with cell cycle regulation.

The STGC3 protein is mainly found in the nucleus, where protein expression is mainly controlled. Proteomic analysis is a powerful tool for global evaluation of protein expression, and it has been widely applied in analysis of disease states, particularly in the field of cancer research. Differential profiling of protein expression by 2-DE is a crucial part of proteomics. The technique can provide reproducible differential expression values for proteins in 2 or more biological samples. In the present study, we identified 9 differentially expressed proteins from *STGC3* over-expressed xenografts in female and male mice. Among these proteins, emphasis was given to Hsc70, which is involved in the regulation of cell cycle regulation.

We confirmed that *STGC3* decreased Hsc70 and its downstream factor cyclin D1, which cause the G_0 and G_1 phase cell arrest, using Western blotting. The Hsc70 family contains both heat-inducible and constitutively expressed members (Garbuz et al., 2011). The latter are the heat-shock cognate proteins. Hsc70 belongs to the heat-shock cognate subgroup. This protein binds to nascent polypeptides to facilitate correct protein folding. It also functions as an ATPase in the disassembly of clathrin-coated vesicles during transport of membrane components through the cell. Hsc70 associates with newly synthesized cyclin D1 and is a component of a mature, catalytically active cyclin D1/CDK4 holoenzyme complex (Diehl et al., 2003). Cyclin D1 mediates G_1-S phase cell cycle progression through activation of specific cyclin-dependent kinases that phosphorylate the retinoblastoma protein, thereby alleviating repression of E2F-DP transactivation of S-phase genes (Masamha and Benbrook, 2009). Loss of cyclin D1 can cause G_1 phase cell arrest in some cells (Masamha and Benbrook, 2009). Cyclin D1 is overexpressed in a variety of cancers and is associated with tumorigenesis and metastasis. Furthermore, cyclin D1 activates estrogen receptor-mediated transcription in the absence of estrogen and enhances transcription in its presence (Zwijsen et al., 1997). This evidence is consistent with the finding that *STGC3* inhibits tumor growth more in female mice than in male mice.

The *STGC3*-associated differential proteins identified are involved in cell cycle regulation, the cytoskeleton, cell metabolism, and signal pathways. The effect of the sexually dimorphic *STGC3* inhibition in CNE2 cells was associated with G_0/G_1 cell arrest through down-regulation of Hsc70 and cyclin D1. It is reasonable to predict that *STGC3* plays an important role in suppressing tumorigenesis in NPC, which also exhibits sexual dimorphism. The findings reported here provide a basis to comprehensively investigate the precise molecular mechanism of *STGC3* in the tumor suppression process. Considering the sexual dimorphism of *STGC3* and the 3:1 male predominance in the incidence of NPC, our results also support continued basic or clinical research in NPC using cell models from female patients, and female animal models.

REFERENCES

Abdel Khalek Abdel RA and King A (2012). MRI and CT of nasopharyngeal carcinoma. *AJR Am. J. Roentgenol.* 198: 11-18.

Chae JI, Kim J, Woo SM, Han HW, et al. (2009). Cytoskeleton-associated proteins are enriched in human embryonic-stem cell-derived neuroectodermal spheres. *Proteomics* 9: 1128-1141.

Chong VF and Ong CK (2008). Nasopharyngeal carcinoma. *Eur. J. Radiol.* 66: 437-447.

Diehl JA, Yang W, Rimerman RA, Xiao H, et al. (2003). Hsc70 regulates accumulation of cyclin D1 and cyclin D1-dependent protein kinase. *Mol. Cell Biol.* 23: 1764-1774.

Garbuz DG, Astakhova LN, Zatsepina OG, Arkhipova IR, et al. (2011). Functional organization of hsp70 cluster in camel (*Camelus dromedarius*) and other mammals. *PLoS One* 6: e27205.

He XS, Xiao ZQ, Chen ZC, Zhao SP, et al. (2004). Molecular cloning and functional analysis of STGC3 - a novel gene on chromosome 3p21. *Ai Zheng* 23: 1110-1115.

He XS, Deng M, Yang S, Xiao ZQ, et al. (2008). The tumor supressor function of STGC3 and its reduced expression in nasopharyngeal carcinoma. *Cell Mol. Biol. Lett.* 13: 339-352.

Jensen EV (1966). Mechanism of estrogen action in relation to carcinogenesis. *Proc. Can. Cancer Conf.* 6: 143-165.

Jensen EV (2005). The contribution of "alternative approaches" to understanding steroid hormone action. *Mol. Endocrinol.* 19: 1439-1442.

Jensen EV, Suzuki T, Kawashima T, Stumpf WE, et al. (1968). A two-step mechanism for the interaction of estradiol with rat uterus. *Proc. Natl. Acad. Sci. U. S. A.* 59: 632-638.

Li L, He XS, Luo QA, Zhang ZW, et al. (2011). Effect of STGC3 gene deletion mutant on the growth of CNE2 cells. *Prog. Biochem. Biophys.* 38: 248-253.

Masamha CP and Benbrook DM (2009). Cyclin D1 degradation is sufficient to induce G1 cell cycle arrest despite constitutive expression of cyclin E2 in ovarian cancer cells. *Cancer Res.* 69: 6565-6572.

Pollard PJ, Briere JJ, Alam NA, Barwell J, et al. (2005). Accumulation of Krebs cycle intermediates and over-expression of HIF1alpha in tumours which result from germline FH and SDH mutations. *Hum. Mol. Genet.* 14: 2231-2239.

Powers MV, Clarke PA and Workman P (2008). Dual targeting of HSC70 and HSP72 inhibits HSP90 function and induces tumor-specific apoptosis. *Cancer Cell* 14: 250-262.

Qiu QC, Hu B, He XP, Luo Q, et al. (2012). STGC3 inhibits xenograft tumor growth of nasopharyngeal carcinoma cells by altering the expression of proteins associated with apoptosis. *Genet. Mol. Biol.* 35: 18-26.

Takatani T, Takaoka N, Tatsumi M, Kawamoto H, et al. (2001). A novel missense mutation in human lactate dehydrogenase B-subunit gene. *Mol. Genet. Metab.* 73: 344-348.

Wang HY, Sun BY, Zhu ZH, Chang ET, et al. (2011). Eight-signature classifier for prediction of nasopharyngeal [corrected] carcinoma survival. *J. Clin. Oncol.* 29: 4516-4525.

Xiong W, Zeng ZY, Xia JH, Xia K, et al. (2004). A susceptibility locus at chromosome 3p21 linked to familial nasopharyngeal carcinoma. *Cancer Res.* 64: 1972-1974.

Yoneda K, Rokutan K, Nakamura Y, Yanagawa H, et al. (2004). Stimulation of human bronchial epithelial cells by IgE-dependent histamine-releasing factor. *Am. J. Physiol. Lung Cell. Mol. Physiol.* 286: L174-L181.

Yu MC and Yuan JM (2002). Epidemiology of nasopharyngeal carcinoma. *Semin. Cancer Biol.* 12: 421-429.

Zhang J, Liu W, Liu J, Xiao W, et al. (2010). G-protein β2 subunit interacts with mitofusin 1 to regulate mitochondrial fusion. *Nat. Commun.* 1: 101.

Zwijsen RM, Wientjens E, Klompmaker R, van der Sman J, et al. (1997). CDK-independent activation of estrogen receptor by cyclin D1. *Cell* 88: 405-415.